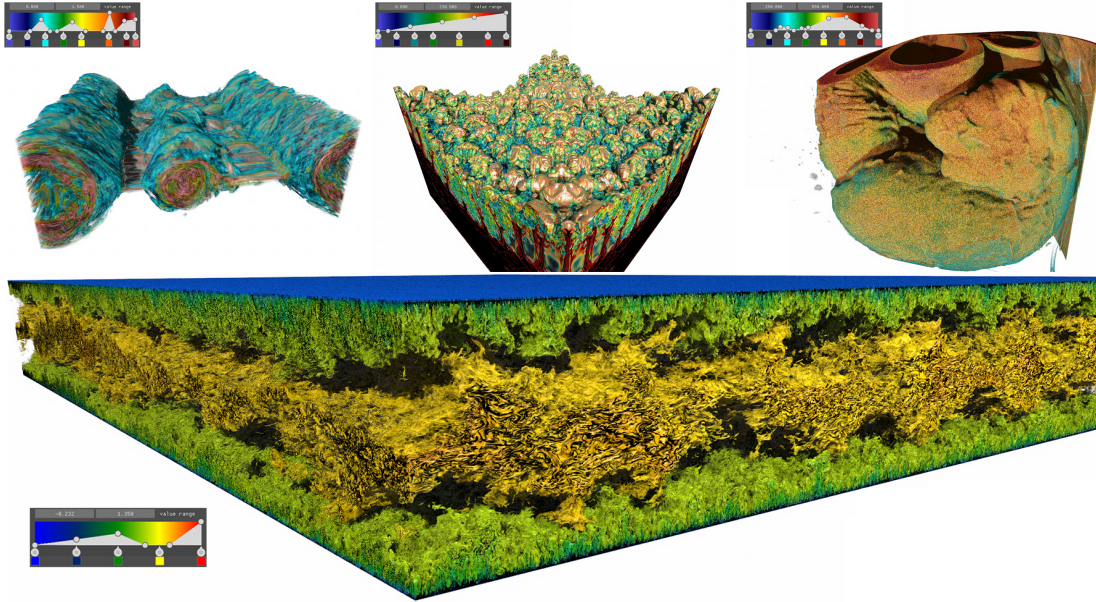


# Interactive Rendering of Large-Scale Volumes on Multi-Core CPUs

Category: Research



**Figure 1:** Screenshots from our high-fidelity interactive volume visualization renderer. Top left: volume rendering of a  $512^3$  magnetic reconnection dataset [16]. Top middle: volume rendering of the  $2048 \times 2048 \times 1920$  Richtmyer-Meshkov instability (RMI) [6]. Top right: visualization of a  $2048 \times 2048 \times 2612$  cardiac volume [22]. Bottom: visualization of the  $10240 \times 7680 \times 1356$  DNS dataset [31]. All images are rendered with surface shading.

## ABSTRACT

Recent advances in large-scale simulations have resulted in volume data of increasing size that stress the capabilities of off-the-shelf visualization tools. Users suffer from long wait times because large data must be read from disk into memory prior to rendering the first frame. In this work, we present a volume renderer that enables high-fidelity interactive visualization of large volumes on multi-core CPU architectures. Compared to existing CPU-based visualization frameworks, which take minutes or hours for data loading, our renderer allows users to get a data overview in seconds. Using a hierarchical representation of raw volumes and ray-guided streaming, we reduce the data loading time dramatically and improve the user's interactivity experience. We also examine system design choices with respect to performance and scalability. Specifically, we evaluate the hierarchy generation time, which has been ignored in most prior work, but which can become a significant bottleneck as data scales. Finally, we create a module on top of the OSPRay ray tracing framework that is ready to be integrated into general-purpose visualization frameworks such as Paraview.

**Index Terms:** Human-centered computing—Visualization—Visualization techniques—Treemaps; Human-centered computing—Visualization—Visualization design and evaluation methods

## 1 INTRODUCTION

Interactive visualization of large-scale volumetric data, produced by simulations, astronomical instruments and high-resolution sensors, allows research scientists to explore scientific data, validate hypotheses and discover new knowledge [21]. However, the increasing data resolution in current high-performance computing (HPC) simulations can easily surpass the capabilities of host systems, making interactive visualization of such data challenging. First, loading the

full-resolution data into main memory is impractical due to memory limitations. Second, for large datasets, the IO latency incurred by the data loading process is prohibitive in the existing volume renderer, even if all the data fits into memory. The long IO waiting time for large dataset degrades the user experience. Therefore, research on novel techniques for data visualization, processing, storage and IO that scale to extreme-scale data is required to transcend the limitations of current hardware [1].

Current solutions for scalable volume data visualization mostly employ GPU architecture since it has been shown to be effective for interactive visualization. Prior studies [8, 10, 19] have applied out-of-core approaches, level-of-detail (LOD) techniques, progressive rendering and data compression schemes to overcome GPU memory limitations. However, these approaches inevitably employ extra data structures (e.g., page tables) and incur frequent CPU-GPU communication to refine the visible data, which hampers the interactivity. Some studies also consider architectures employing CPUs since the amount of memory directly accessible by a CPU often dwarfs the amount of VRAM available on even the most powerful GPUs. Previous studies have shown that an optimized CPU volume renderer can outperform a GPU renderer for sufficiently large volumes [23, 36, 39]. However, several studies [3, 20, 32] have focused on distributed parallel rendering on supercomputers, but very few have addressed interactive visualization of large-scale volumes on a single workstation.

In this work, we present an interactive visualization solution for large-scale volumes on multi-core CPU architectures. Our solution allows users to get an overview of the large data in seconds rather than minutes or hours using existing visualization frameworks. We build our approach on a hierarchical data structure – *Bricktree* – that allows for a hierarchical representation of the volume. During the

rendering, we stream the necessary data on demand with separate threads and employ ray-guided progressive rendering for data refinement. As an extension of the OSPRay ray tracing framework, which already contains various techniques for visualizing scientific data [39, 43], we build a Bricktree module along with an efficient hierarchy generation tool to support large-scale data visualization on multi-core workstations. Given that OSPRay has been integrated into Paraview and VisIt, our module is ready to be integrated into general-purpose visualization frameworks. Specifically, our contributions in this paper are:

- An interactive visualization solution for large-scale volume visualization, which decouples the data loading and rendering process on multi-core architectures and dramatically reduces the amount of time the user has to wait before being able to explore the data.
- The Bricktree, an efficient and low-overhead hierarchical structure that allows for encoding a large volume into a multi-resolution representation. We also evaluate the structure with several choices of parameters.
- An OSPRay module for large data visualization and a parallel hierarchy generation tool that are ready to be "dropped into" a general-purpose visualization pipeline.

## 2 PREVIOUS WORK

Although widely used for visualization of 3D scalar fields, volume rendering remains a computation, memory and I/O-intensive task [44]. Several studies have focused on improving the rendering performance by introducing efficient packet BVH traversal [23, 39], empty space skipping [17] and early ray termination [25, 28]. Although efficient for visualizing moderate-size volumes on consumer desktops, these methods struggle to scale to petascale or exascale datasets since they assume that the entire volume is present in memory. Previous work on large-scale volume rendering can be categorized as:

1) Parallel/distributed rendering on distributed memory systems. These approaches parallelize data processing over many nodes [4]. Research has demonstrated strong scalability on both CPU and GPU clusters [2, 3, 9, 13, 20, 32]. For example, Howison et al. [20] demonstrated that MPI-hybrid parallelism achieves a sublinear raycasting speed-up and is more efficient in terms of overall speed and memory than the MPI-only parallelism. However, previous work [44] has found that the main performance bottleneck of distributed visualization lies in final image compositing rather than in the volume rendering process.

2) Visualization of large-scale volumes on a stand-alone workstation. Much effort has been devoted to the implementation of GPU renderers due to the great hardware interpolation capabilities [5, 11]. Beyer et al. [1] conducted a detailed survey on this topic. Most prior work focuses on overcoming the GPU's memory limitation and tackling this issue by loading only the visible part of the volume into GPU memory [29]. The GigaVoxels system [7, 8], the first to employ this idea, determines the visibility of small blocks "on the fly". Although capable of rendering several billion voxels in real-time, it mainly focuses on entertainment applications and targets sparse volume datasets. CERA-TVr [10] then extended the GigaVoxel paper, targeting scientific visualization user cases. In contrast to GigaVoxel, CERA-TVr is capable of rendering dense volumes and can progressively refine parts of a framebuffer if the size of the visible data exceeds the size of the brick pool. Hadwiger et al. [18] proposed a virtual memory scheme that avoids explicit tree traversal and supports interactive visualization and streaming of petascale 2D image data. However, this approach exhibits IO latency during 3D block construction due to cache misses and requires that all visible

data fit into cache. All these approaches inevitably require heavy CPU-GPU communication, which significantly impacts interactivity.

In the context of the CPU-based renderers, very little research has focused on large-scale volume rendering on multi-core workstations. As a state-of-art CPU ray-tracing framework for scientific visualization, OSPRay works well for interactive visualization of moderate-size volume data and can potentially be extended to large-scale data. Wu et al. [44] proposed the VisIt-OSPRay system, which can scale to large-scale datasets. To achieve interactive visualization, they integrated OSPRay into VisIt as a backend visualization toolkit and coupled it with PIDX (parallel IO library) [26] for scalable IO. This study achieved interactive visualization, but it took more than 30 minutes to load the DNS dataset into memory with 64 processors on Stampede2.

To address these challenges, we decompose large volumes into a hierarchical representation, with each node representing a small cubic brick. Within the rendering pipeline, we leverage ray-guided streaming and progressive rendering to reduce IO latency.

## 3 BRICKTREES

Adaptive space subdivision and hierarchical data representation are key to interactive visualization of large-scale volumetric datasets [8]. These techniques enable us to load and update the working set on demand to address IO latency and memory limitations. As a popular hierarchical data structure for 3D space subdivision, the octree has been well studied for direct volume rendering [15]. Hierarchical grids feature a theoretically optimal number of traversal steps, and thus have been overtaken as general-purpose ray tracing acceleration structures [24]. Lefebvre et al. [27] proposed the  $N^3$ -tree, which is capable of dividing each edge by an arbitrary number N rather than 2.  $N^3$ -tree was later used in the GigaVoxel system [8]. Other structures, such as kd-trees, are also used in isosurface rendering with the trend of coherent ray tracing [34, 38, 40].

In this work, we define a hierarchical data structure – "Bricktree" – which allows us to represent a structured volume in a hierarchical, multiresolution and compressed way (as shown in Figure 2). Rather than encoding the large volume into a single deep Bricktree, our design tiles the volume into a "Bricktree Forest" which consists of a list of Bricktrees. This design is not only conducive to parallel tree traversal on multi-core CPU architectures, but also avoids encoding a large empty space when the structured volume is not a perfect cube ( $M \neq L \neq K$ ). A Bricktree is a generalization of an octree where we subdivide a node by an arbitrary number  $N^3$  rather than by 8. Furthermore, a Bricktree is similar to an  $N^3$ -tree but with an arbitrary branching factor  $N^3$  rather than by 8 (as shown in Figure 3).

### 3.1 Data Layout

In our design, a "brick" is an  $N \times N \times N$  set of cells. Obviously, each cell can store a data value. We denote a brick that stores data values as a "Valuebrick". Bricks can be thought of as nodes of a tree with branching factor  $N^3$ . We call such a tree a "Bricktree". Each brick can have up to  $N^3$  children, where each child brick is associated with exactly one cell in the parent brick. If a brick does have children, the child indices are stored in an "Indexbrick". Thus, we represent a brick as a Valuebrick and an optional Indexbrick in memory. Also along with a indexBrickID to indicate the corresponding relationship between the Valuebrick and the Indexbrick.

Each cell of a Valuebrick corresponds to a set of voxels in the volume. For a "leaf brick" (e.g.  $N_{16}$ ), one cell corresponds to exactly one voxel and the cell's value equals to the value of this voxel. By contrast, each cell of an "inner brick" (e.g.  $N_0$ ) typically represents a set of voxels. Accordingly, we can assign a value to each cell by averaging over all voxels in this set. Each cell of an Indexbrick refers to a child brick the current brick has children. For a "leaf brick", it has no children and thus no Indexbrick. In this case, the

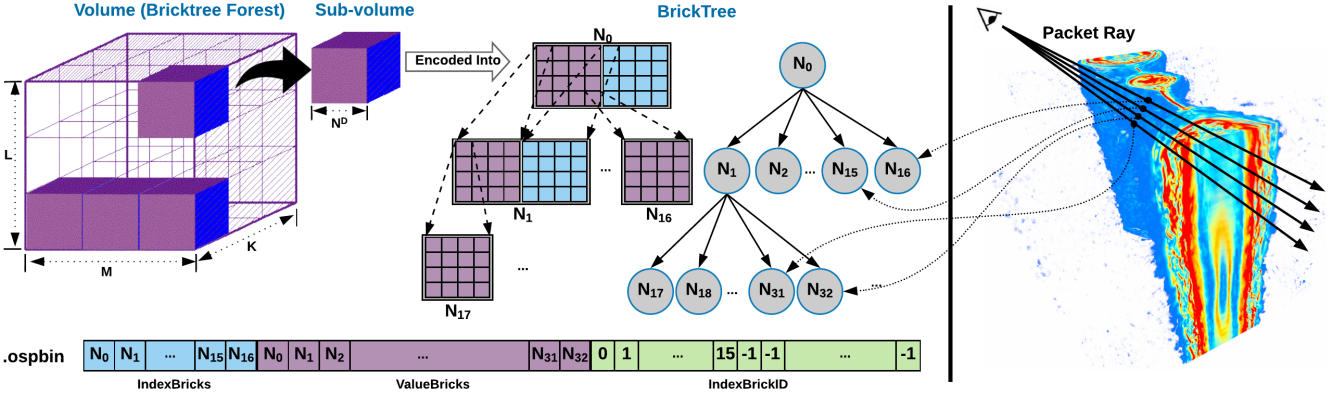


**Figure 2:** An illustration of the layout of the Bricktree structure. Each brick (e.g.  $N_0, N_1\dots$ ) is represented with a Valuebrick (colored in purple), an indexbrick and an optional Indexbrick (colored in light blue). The indexbrick stores the index of the Indexbrick if a node has one. Otherwise, -1 is stored. Both Valuebricks and Indexbricks contain  $N^3$  cells. Each cell encodes a float value in a Valuebrick or an int32 reference in an Indexbrick.

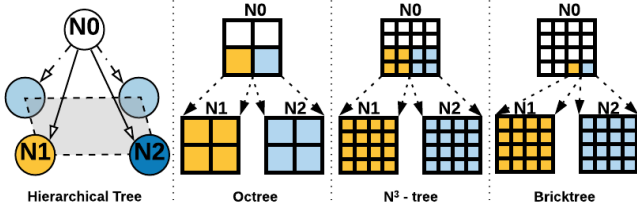


**Figure 3:** Comparison of an octree, a  $N^3$ -tree and a Bricktree(2D representation). In a 3D scenario, an octree has a branching factor of  $2^3$  and allows for decomposing a node into  $2^3$  cells; A  $N^3$ -tree has a branching factor of  $2^3$  and allows for decomposing a node into  $N^3$  cells; A Bricktree has a branching factor of  $N^3$  and allows for decomposing a node into  $N^3$  cells.

indexbrickID of this brick is set to invalid (-1). While for a “inner brick”, its indexbrickID refers to the right Indexbrick and the cells in this Indexbrick point to the children. In Figure 2, a Valuebrick is shown in purple and an Indexbrick is in light blue.

Multiple Bricktrees can be combined to form a “Bricktree Forest”. Recall that this allows us to tile a nonsquare domain efficiently. Figure 2(left) illustrates a structured volume with dimension of  $M \times L \times K$ , which is organized into a BrickTree Forest. Each Bricktree is specified through a brick size ( $N$ ), a data type ( $T$ ) and a tree depth ( $D$ ), and represents a set of  $N^D \times N^D \times N^D$  voxels in the volume.

In memory, each  $\text{BrickTree } < N, T >$  is represented as three linear arrays:

1. One linear array of Valuebricks, where each Valuebrick contains  $N \times N \times N$  values of type  $T$ .
2. One linear array of int32 “indexbrickIDs”, with exactly one such int32 per Valuebrick. If a given Valuebrick’s indexbrickID is invalid, it does not refer to an Indexbrick and thus has no children; otherwise, this ID refers to an Indexbrick in the Indexbrick array.
3. One linear array of “Indexbricks“, where each Indexbrick contains  $N \times N \times N$  int32 indices. Each such index can be invalid (meaning the corresponding cell does not have a child); if the index is greater than or equal to 0, it refers to a brick in the Valuebrick array.

On a file system, the whole volume is represented by one “.osp” file that contains meta-data ( $N, T, (M, L, K)$  of input volume, etc). Each Bricktree is stored in two files: 1) an “.osp” file that gives high-level information ( $N, T, D$ , etc.) in XML form; 2) an “.ospbin” file that contains the three arrays in binary form.

### 3.2 Bricktree Overhead

Due to the specific layout, our Bricktree is easy to index and the overhead is low. Given a Bricktree with a brick size of 4, a data type of float and a depth of 4 ( $\text{Bricktree } < 4, \text{float} >$ ), a certain number of  $4^3$  Valuebricks and  $4^3$  Indexbricks will be generated when building the tree. In practice, leaf Valuebricks have zero overhead, since each costs exactly 256 bytes for 64 float-typed cells. The only overhead lies in the Indexbricks and inner Valuebricks. However, few of these bricks exist relative to the number of leaf bricks (see Figure 4).

In a more ideal case, where many of the inner nodes all point to the leaf Valuebrick, we store only about one 32-bit int (4 byte) for a complete leaf Valuebrick. Hence, 4 bytes are used to index 256 “payload” bytes for float data. A less ideal case is that some children of inner nodes are leaves, while other children are inner nodes. Recall that for each inner node, we need to store both a Valuebrick and an Indexbrick. This will result in more memory consumption than in the ideal case. However, the overhead will still most likely be considerably less than that of an octree. Benchmarks in Table 1 show that the in-memory size of a Bricktree with  $N = 4$  is much smaller than a Bricktree with  $N = 2$ , which is an octree. In addition, few bricks are located in the upper levels of the tree. Assuming a brick size of 4, the number of inner nodes goes down by a factor of 64 each time we go up one level in the tree. This holds in practice - the overhead of Bricktree with  $N = 4$  is 8.0% on the magnetic reconnection dataset (see Figure 8) and the DNS dataset (see Table 1). By contrast, the overhead of octree (Bricktree with  $N = 2$ ) is 43% and 72% respectively.

### 3.3 Hierarchy Generation in Parallel

As an offline process that is usually run in advance, the performance of reorganizing the volume into multi-resolution bricks is mostly ignored in the volume rendering literature [14]. However, it becomes a significant bottleneck for large-scale datasets. As illustrated in [14], the runtime for building a hierarchical structure for RMI (8.1 GB,  $2048 \times 2048 \times 1920$ ) is up to 1.5 hours in the worst case and 13 minutes in the best case. Petascale datasets might take hours or days. The virtual memory architecture of [18] alleviates this problem by constructing the brick at runtime. However, the latency

of constructing bricks at runtime will dramatically influence the framerate, especially when the visible data is missing in memory.

Our design also makes hierarchy generation more efficient. It is straightforward that we can construct the Bricktree Forest in parallel. The “*ospRawToBricks*” tool, which employs the *GNU make* command, is used to meet this end. Normally, *make* will execute only one recipe at a time. By specifying the “*-j*” option, it is possible to execute many recipes simultaneously. Once parameters *N*, *T* and *D* are set, we first generate an index file over the Bricktrees as well as a makefile. The makefile is used to build each Bricktree in parallel. See Algorithm 1 for the algorithm used to recursively construct a Bricktree. Measurements of the performance improvement from parallelization are shown in Figure 9.

---

**Algorithm 1** The recursive function for constructing a Bricktree. *N, T* is defined as a template parameters. *Threshold* is a customized parameter for “compression”.

---

**Input:** *llC* - left lower coord; *lvl* - tree level; *lvlWidth* - level width.  
**Output:** *avgValue* - average value of a brick; *vRange* - value range.

```

1: function BUILDREC(avgValue, llC, lvl, lvlWidth)
2:   cellSize  $\leftarrow$  lvlWidth/N
3:   brick, vRange
4:   if levelWidth == N then
5:     brick.value[i][j][k]  $\leftarrow$  input.get(N*llC + offset)
6:     vRange.extend(brick.value[i][j][k])
7:   else
8:     lowerLeft  $\leftarrow$  N*llC + offset
9:     vRange  $\leftarrow$  BuildRec(avgValue, lowerLeft, lvl + 1, cellSize)
10:    brick.value[i][j][k]  $\leftarrow$  (T)avg
11:    avgValue  $\leftarrow$  brick.ComputeWeightedAverage()
12:    if vRange  $\leq$  threshold then
13:      This is a brick with each cell of same value.
14:      Kill this brick (value has been saved in parent node).
15:    else
16:      Set this brick into the brick buffer.
return vRange
```

---

In addition, our tree construction approach also supports data format conversion and compression. We can easily convert an input data format to an interval format, such as double to float. Furthermore, we allow the user to set a threshold (*t*) that determine which input regions can be safely collapsed into a single node. For instance, consider a cell *C* with a child brick *B*. Let *Value(b)* be a function that obtains the value at cell *b*  $\in$  *B*, and *t* be the threshold:

$$\left( \max_{b \in B} Value(b) \right) - \left( \min_{b \in B} Value(b) \right) \leq t \quad (1)$$

If Equation 1 holds, then *B* and its children are “collapsed” into *C*, meaning that *C* no longer points to a child brick, and is instead assigned the average value of all cells in *B*. Our default value of *t* is 0, meaning that by default, our implementation losslessly eliminates equal-value regions. This process is also known as “empty space skipping”.

#### 4 VOLUME INTEGRATION

In this section, we illustrate the rendering pipeline with Bricktrees in a simple case where all data have been read into memory. Raycasting-based volume rendering consists of marching rays through the volume with a step size and accumulating color and opacity along the ray. With a hierarchical structure, rays need to traverse the structure until reaching a leaf node, an inner node with appropriate level-of-detail in current view or an unmapped node.

For a given sample point *p* along a ray, we need to query the value of eight neighboring voxels for interpolation. For each voxel, a tree traversal is needed to fetch the Valuebrick that the voxel belongs

---

**Algorithm 2** Pseudocode on sampling a given point *p* and traversal of the Bricktree structure

---

```

1: procedure BT_CPLUS_SAMPLE(p)
2:   valueArray[8]  $\leftarrow$  0
3:   voxelCoord[8]  $\leftarrow$  Calculate 8 vertex's coordinates
4:   while i < 8 do
5:     bTreeID  $\leftarrow$  ComputeBrickTreeID(voxelCoord[i])
6:     bt  $\leftarrow$  GetBrickTree(bTreeID)
7:     valueArray[i]  $\leftarrow$  Bt_Cplus_GetVoxels(bt, voxelCoord[i])
8:     result  $\leftarrow$  lerp(valueArray[8])
9:   return result
10:  procedure BT_CPLUS_GETVOXELS(bt, coord)
11:    brickID  $\leftarrow$  0 ▷ top-down traversal
12:    brickStack.push(brickID)
13:    while brickStack is not empty do
14:      cBrickID  $\leftarrow$  brickStack.pop()
15:      ibID  $\leftarrow$  bt.brickInfo[cBrickID].indexBrickID
16:      cOffset  $\leftarrow$  ComputeOffset(coord)
17:      childBrickID  $\leftarrow$  bt.indexBrick[ibID].child[cOffset]
18:      if childBrickID == -1 then
19:        return bt.valueBrick[cBrickID].child[cOffset]
20:      else
21:        brickStack.push(childBrickID)
```

---

to. We start the Bricktree traversal from the root node. Assume that we operate on brick 1 of a *BrickTree*  $<$  4, float  $>$  and want to know if its cell (1, 1, 2) has a child. First, we look up the brick’s index brick ID (*ibID* = *indexBrickID*[1]). We know that none of the cells of brick 1 have a child if the *ibID* is invalid or less than 0. If this is the case, cell (1, 1, 2) certainly does not have a child. However, if *ibID*  $\geq$  0 (e.g., *ibID* = 1 in Figure 2), then we look at *cellChildID* = *IndexBrick[ibID].child[1][1][2]*. If this value is invalid (-1), then this particular cell of brick 1 does not have any children. Otherwise, *valueBrick[cellChildID]* is the child brick.

Algorithm 2 describes the general sampling process. Trilinear interpolation of eight nodal value is used to determine the value of an arbitrary point *p*. *Bt\_Cplus\_GetVoxels* traverses the Bricktree and queries the value of a given cell.

So far, we have obtained a sample kernel that has access to the Bricktree “forest” and is implemented with C++ code. However, as a loadable module to the OSPRay ray tracing framework, our Bricktree module employs the OSPRay rendering pipeline, which is internally built on top of Embree [41] and ISPC [33]. Embree is a collection of high-performance ray tracing kernels. The Intel SPMD Program Compiler (ISPC) allows a number of program instances to execute in parallel on SIMD hardware. ISPC compiles its own programming language (a variant of C), and this ISPC code can call and be called from C/C++ application code. In OSPRay, the sampling process maps well to the SIMD paradigm, and is thus implemented with ISPC code. Under this condition, we can have two approaches to implement our sampling process.

#### 4.1 C/C++ Serial Implementation

A simple but inefficient approach is a serial implementation with C/C++ code without maintaining a copy of the Bricktree structure on the ISPC side. We can easily implement a C/C++ version of the sample function (see algorithm 2) that has direct access to the Bricktree structure, and call it serially from the ISPC sample callback function. The *foreach active* construct is utilized to specify a loop that iterates over the active program instances serially. The loop executes once for each active program instance, and with only that program instance executing. Algorithm 3 depicts the process of serially calling the C/C++ implementation of sampling function from the ISPC code (*programCount*, *programIndex*, *lane* are built-in

variables in ISPC).

**Algorithm 3** Pseudocode for serially calling the C++ version of sampling function from ISPC code.

---

```

1: procedure BT_ISPC_SAMPLE(varying samplePos)
2:   uniform uPos[programCount]
3:   uniform uValue[programCount]
4:   uPos[programIndex]  $\leftarrow$  samplePos
5:   foreach_active(lane) do
6:     uValue[lane]  $\leftarrow$  Bt_Cplus_Sample(uPos[lane])
7:   return uReturnValue[programIndex]
```

---

## 4.2 ISPC Vectorized Implementation

A more efficient method involves maintaining a sibling Bricktree structure and implementing a parallel tree traversal algorithm that is run on multiple vector instruction set architectures. This method is feasible due to the ISPC code and C/C++ code being able to share the same memory. In this work, we implemented an efficient packet-based variant of *Bt\_ISPC\_GetVoxels* kernel, which is suitable for packet-based ray-tracing on multi-core CPU. We maintained a stack to query the Valuebrick for an entire packet of ray samples. Assuming eight inputs in a packet, the ideal case is all the inputs will traverse to the same Valuebrick, in which case we can achieve a theoretical 8x performance improvement. In practice, not all samples will traverse to the same level, and performance is influenced by Valuebrick size. We achieved a 2x performance improvement for  $N = 4$ .

## 4.3 64-bit Addressing

For performance reasons, ISPC uses 32-bit addressing by default, even with a 64-bit compilation target. In this addressing mode, ISPC maps all addresses for **varying** array access to vectors of 32-bit offsets relative to a shared 64-bit base pointer. However, this approach limits the volume size to 4 GB. When our data exceeds 4 GB, 32-bit addressing will fail in algorithm 2, line 19. Hence, we need to treat each array as consisting of smaller segments, and then iterate over all unique segments addressed by a vector using ISPC's **foreach\_unique** statement. To do so, we can guarantee that each segment can be addressed with a 32-bit offset. More details about the implementation can be found in [37].

By employing this technique, our implementation can scale to the workstation's available memory. However, the implementation has some performance penalties, because 64-bit addressing is slightly more costly than 32-bit addressing. In an ideal case, memory accesses are mostly coherent, and only a few iterations of the aforementioned loop are necessary. **In the worst case, many iterations are needed. However, the performance is still superior to the performance when we recompile our application in 64-bit.**

## 4.4 Sampling Optimization

Although we implement an efficient traversal kernel for packet sampling along the ray, eight neighboring voxels need to be accessed to perform trilinear interpolation. A naive way to access these voxels is to call the traversal kernel eight times. Given that the neighboring voxels are likely located in the same Valuebrick, duplicated traversal can be avoided if we initialize neighboring voxels in the same Valuebrick.

Ideally, only one traversal of the Bricktree rather than eight is needed for a given sample point. In practice, the speed-up is lower than 8x, since we need to re-traverse the tree for the neighboring voxels that are located in neighboring Valuebricks. Some solutions avoid the re-traverse by replicating a layer of ghost voxels at the brick's boundary, which is a trade-off between time and space. For large datasets, data overhead with this approach will be high when

a small brick size is used. Benefiting from the large branching factor of our data structure, the generated Bricktrees will keep a small tree depth. Hence, the re-traversal at the brick boundary will only slightly impact the performance. One would expect to achieve a higher speed-up with a larger brick size, but larger brick sizes incur more possibility that eight voxels are located in the same brick but with inefficient empty space skipping [14]. An analysis of the choice of brick size is conducted in Section 6.2. By performing the optimization mentioned above, we achieve a 4-5x performance improvement for  $N = 4$ .

**Algorithm 4** Sampling function with progressive rendering on top of our Bricktree structure

---

```

1: procedure BT_ISPC_GETVOXELS(bt, coord)
2:   cBrickID  $\leftarrow$  0                                 $\triangleright$  current brick, set to root
3:   pBrickID  $\leftarrow$  -1                                $\triangleright$  parent brick
4:   uniform FindStack stack[16]                       $\triangleright$  ISPC stack struct
5:   stackPtr  $\leftarrow$  pushStack(&stack[0], cBrickID, pBrickID)
6:   while stackPtr > stack do
7:     -- stackPtr
8:     if stackPtr is active then
9:       cBrickID  $\leftarrow$  stackPtr.cBrickID
10:      pBrickID  $\leftarrow$  stackPtr.pBrickID
11:      if current brick is not requested then
12:        bt.brickStatus[cBrickID].isRequested  $\leftarrow$  true
13:
14:      if bt.brickStatus[cBrickID].isLoaded then
15:        childBrickID  $\leftarrow$  getChildBrickID()
16:        cOffset  $\leftarrow$  ComputeOffset(coord)
17:        if childBrickID = -1 then
18:          return value in current brick
19:        else
20:          stackPtr
21:          pushStack(stackPtr, childBrickID, cBrickID)            $\leftarrow$ 
22:        else
23:          return average value in parent brick
```

---

## 5 RAY-GUIDED PROGRESSIVE RENDERING

The long waiting times of loading data from disk significantly influence the user experience in an interactive visualization. In this section, we describe the solution to reducing IO latency with data streaming and progressive rendering. Data streaming and rendering are decoupled in our visualization pipeline. If requested data is not yet in memory, the renderer uses the average value stored in the (already loaded) parent node and requests the missing brick from a data loading thread. Consequently, the visualization process can be

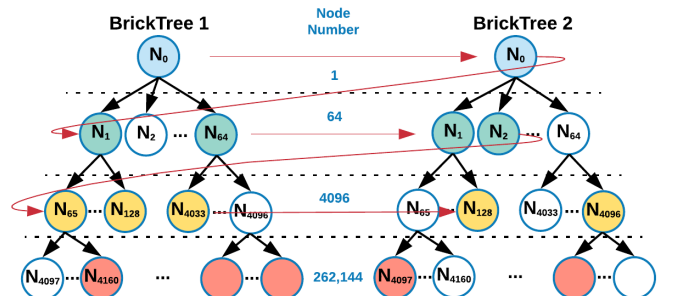


**Figure 4:** An illustration of streaming the Valuebrick by level. Colored nodes are requested in current time. The red arrow indicates the loading sequence.

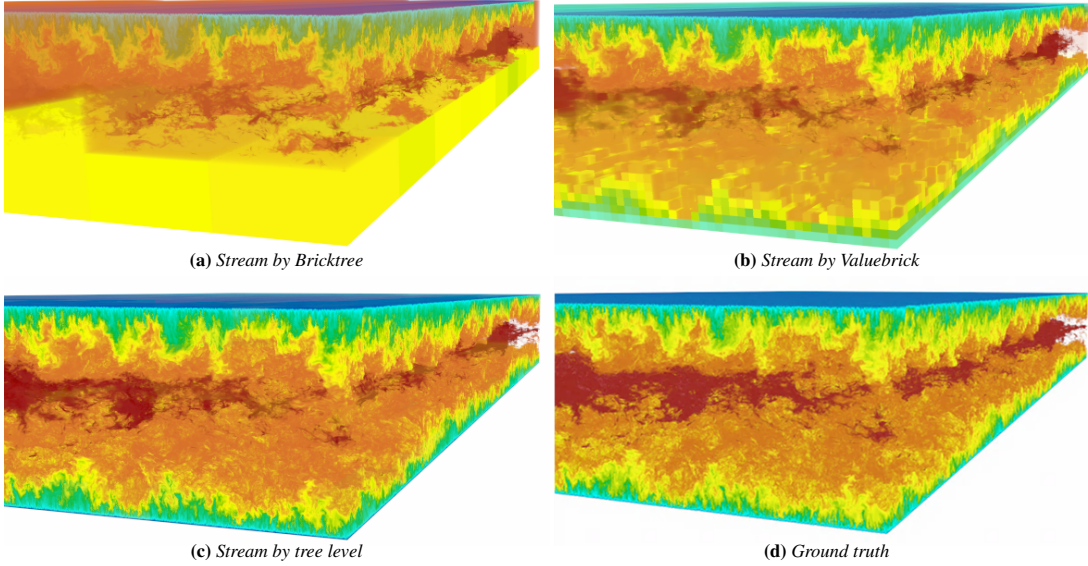


**Figure 5:** A comparison of rendering image of the DNS dataset with three Valuebrick loading strategies at frame 100. Stream by level shows more detail and smoother data refinement.

launched very quickly without waiting for the large data to first be loaded into the memory. In addition, rendering performance remains stable when the camera position is updated.

### 5.1 Valuebrick Streaming

So far, we have illustrated how we sample and traverse the Bricktree assuming that all multiresolution bricks are in memory, which works well on small- or moderate-size datasets. For large datasets, however, IO bottlenecks and memory size limit performance and rendering quality. In particular, IO latency for loading the dataset into memory before rendering becomes prohibitive when visualizing large data. Loading a terascale dataset into memory on a contemporary workstation might take hours, even with a parallel IO library such as PIDX. Furthermore, the memory might not be adequate to load all bricks.

To solve this problem, we employ ray-guided progressive rendering and stream bricks on demand. Although the idea behind this approach is similar to GigaVoxel [8] and to Hadwiger’s work [18], our implementation on multi-core CPUs is more straightforward, and it avoids CPU-GPU communications and the complex data structures needed to store the rendering context. As mentioned in Section 3.1, each Bricktree stores a linear array of Valuebricks. All we need to do is maintain a status for each Valuebrick and update it correctly according to the rendering context. In our solution, the *isrequested* and *isloaded* flags are used to identify the current status of a Valuebrick. In our sample function, the *isrequested* flag of a Valuebrick is set when we need to load the Valuebrick into memory, which allows us to implement a visibility-based solution that requests only data that is inside the view frustum.

#### 5.1.1 Progressive Sampling

The sample function needs to be able to handle the equivalent of a cache miss – the case when a Valuebrick is needed but not in the memory – to generate a correct image. One simple and synchronous approach mentioned in [8] is to load the missing Valuebrick immediately and for volume integration to stop until the Valuebrick is loaded. This approach is unacceptable for interactive visualization when many Valuebricks are missing due to the prohibitive IO latency incurred by Valuebrick loads. Given that the inner node in the Bricktree stores the average values of its child nodes, we adopted an asynchronous approach for volume integration. We use

the average value as an approximation for the current sample point when we request the Valuebrick and refine the output image when the Valuebrick is loaded in separate threads. Algorithm 4 depicts the pseudo-code of this process.

#### 5.1.2 Valuebrick Loading Strategy

In this work, multi-threading is employed to decouple the data streaming and rendering. We create independent threads that are responsible for determining the streaming sequence and loading the requested Valuebrick from the file system. These threads are able to access the Valuebrick buffer and update the *isloaded* status when a Valuebrick is loaded. Coordinated with the progressive sampling, an interactive and smooth visualization is achieved.

Although we achieve a stable framerate by decoupling the data streaming and rendering, the Valuebrick loading sequence impacts the qualitative performance of our progressive refinement strategy. Given the layout of our Bricktree, three choices are considered.

Recall from Section 3.1 that the volume is encoded as a Bricktree Forest. Hence, the naive approach is to map the whole Bricktree into memory if a Valuebrick in the respective Bricktree is requested. We refer to this approach as “streaming by Bricktree”. This approach is easy to implement but not efficient, because Bricktrees tend to be large, and because many unrequested Valuebricks will be loaded.

A finer-granularity approach is to “stream by Valuebrick” rather than by Bricktree. For each Bricktree, the streaming threads will filter and load the requested Valuebricks. This approach yields better performance than the first approach, since loading a Valuebrick is much cheaper than loading a Bricktree. Visually, the user will notice a smoother and finer grained refinement (as shown in Figure 5b). However, for the first few frames, when a large number of Valuebricks are missing, performance is lackluster, since many Valuebricks will be requested at once by the ray sample function. In the worst case, we need to load almost all Valuebricks in the current Bricktree before moving to the next Bricktree, which results in a slight performance improvement over the first approach.

Generally, the data exploration process is “overview first, zoom and filter, then detail-on-demand” [12, 42]. Following this mantra, the ideal approach is to update the data resolution progressively. In this work, we adopt an approach similar to level-order tree traversal and load the requested Valuebricks by level. Figure 4 illustrates this

approach. Given a user-defined view frustum, the streaming thread selects the requested Valuebricks (colored) by level and pushes them into a queue to load. Due to the large branching factor ( $N^3$ ) of our hierarchical structure, only a small portion of the nodes are inner nodes. For example, in Figure 4, using  $4^3$  bricks to encode a  $512^3$  volume, only 1.6% of the nodes are inner nodes. Consequently, loading the inner node levels takes relatively little time, and we can achieve smooth visual refinement of our data. Figure 5 compares visual refinement using different streaming strategies.

Another factor that improves progressive refinement performance is Valuebrick load speed, although this is highly dependent on IO throughput. Due to the design of the Bricktree “forest”, the levels of the Bricktree can be loaded in parallel since each process is independent. For example, we can load level 2 of tree 1 and tree 2 in parallel using `tbb :: tasking_parallel`. Compared to serial streaming, we observe that parallel streaming significantly improves performance.

## 5.2 Early Tree Traversal Termination

So far, we have discussed a ray-guided visibility culling approach that allows our renderer to load only the visible portion of the volume. The idea is, for a given viewport, that only part of the data contributes to the final image. Similar ideas can be applied to improve rendering performance. In particular, under the right conditions, Bricktree traversal can be stopped at an inner node that reaches the appropriate level-of-detail (LOD).

### 5.2.1 Level-of-Detail Control

Some primitives are smaller than the output device pixels when rendering a large dataset at low magnification [35]. Generally, in this case, it is hard to tell the visual difference in the interactive rendering if we use higher resolution data. One general-purpose approach to reduce rendering time is to store data at a discrete level of detail and select a lower resolution LOD with primitives that more closely matches the display resolution.

In this work, it is easy to apply LOD-based ideas since an inner node can be interpreted as a coarser representation of its descendants. During traversal, we calculate the projected screen space area of a Valuebrick and stop the traversal if the area is smaller than a user-defined threshold. To simplify computation, we use a sphere as an approximation of a cubic Valuebrick. By setting the threshold to one pixel, we achieve a 2.5x speed-up when we zoom out and view the DNS dataset at low magnification.

### 5.2.2 Culling with Transfer Function

We can stop the traversal when the Valuebrick does not contribute to the final image given the current transfer function. In general, the performance of interactive visualization depends on the user-defined transfer function. For example, the framerate drops to 2-3 fps if we make the interior of the DNS volume transparent and keep the top and bottom boundaries opaque, because rays terminate much later when most of the volume is transparent. Furthermore, tree traversal is still performed on each sample even when its corresponding Valuebrick is transparent. Taking advantage of the value range stored in each node, this can easily be avoided in our implementation. The callback function `getMaxOpacityInRange(cellRange)` allows us to look up the brick’s maximum opacity based on the current transfer function. If the maximum opacity equals 0, the tree traversal stops at the current Valuebrick and skips the descendants. Although the speed-up of this optimization depends on the data and transfer function, we achieve an average 2x speed-up for the DNS dataset with a transparent interior.

## 6 RESULTS

In this section, we evaluate four key aspects of our system: 1) the performance of the existing OSPRay volume renderer and our Bricktree module; 2) the performance of the Bricktree with different brick

sizes; 3) data compression using the Bricktree; 4) the performance of Bricktree generation. Unless otherwise noted, benchmarks were performed on a quad-socket workstation (FSM) with four Xeon E7-8890 v3 CPUs, with a total of 72 physical cores at 2.5 Ghz, along with 3 TB RAM. All test datasets are stored on a network mounted file server over a 1Gb/s network. The I/O throughput of the file system is 110 MB/s. In the benchmark, volumes were rendered to a  $1024 \times 768$  framebuffer, and the rendering performance was measured by calculating the average framerate over 100 frames. Bricktree read and write bandwidths include effects from the filesystem cache, which may results in measured bandwidt value that appear to exceed the underlying hardware’s capability. Nonetheless, the measured read/write times are the ones that would be observed by a real user.

We tested our renderer with four datasets with sizes ranging from small (e.g., magnetic reconnection volume [16]), to medium (e.g., the Richtmyer-Meshkov instability simulation [6] and cardiac volume [22]) to extremely large (e.g., the DNS dataset [31]).

- The magnetic volume, produced from kinetic simulations, is a  $512^3$  float-precision dataset (size: 512 MB) that represents magnetic reconnection in relativistic plasmas.
- The Richtmyer-Meshkov instability (RMI) is a simulation of carbon hexafluoride being pushed up through a wire mesh, with a resolution of  $2048 \times 2048 \times 1920$  and data type of uint8 (size: 8.1 GB). It is a popular dataset and is also used in [14, 24, 44].
- The cardiac volumes were obtained by way of computed tomography (CT) imaging on excised, postmortem porcine hearts. The resolution of the data is  $2048 \times 2048 \times 2612$ . With a data type of int16, the size of the data goes up to 21 GB.
- The DNS, produced by the Institute for Computational Engineering and Science (ICES) at the University of Texas-Austin is a single  $10240 \times 7680 \times 1536$  double precision volume (size: 900 GB) from a turbulent flow simulation.

## 6.1 Existing OSPRay Renderer vs. Bricktree Module

Although the existing OSPRay volume renderer provides limited support for rendering large volumes on CPU, it can suffer from prohibitive IO latency because all the data must be loaded into memory before the first frame can be rendered.

Figure 6 illustrates the trade-off between overall performance and loading time when volume rendering with our Bricktree module against the pre-existing OSPRay renderer. It is shown that the overall performance of the Bricktree module is around 35% lower compared to the OSPRay renderer, since use of the Bricktree necessitates a hierarchy traversal. By contrast, the existing OSPRay renderer uses a standard structured volume representation, allowing data to be queried using simple math operations. Despite some performane loss, Figure 6a indicates that our Bricktree module still runs at interactive framerates.

More importantly, our Bricktree module performs much better than the existing OSPRay renderer when it comes to loading time. We measured the time that a user must wait before the renderer draws the first frame (see in Figure 6b). The Bricktree module achieves much better performance since it only needs to load metadata prior to rendering. With both renderers, loading time increases with data size. However, our Bricktree module slows down much less. For instance, without the Bricktree module, users must wait more than 20 minutes on the test workstation (FSM) before being able to see a “bird’s eye view” of the DNS dataset. By contrast, with our Bricktree module, the DNS dataset loads in under 40 seconds. Therefore, we believe that the Bricktree module is a better choice for rendering large datasets, while the existing OSPRay volume renderer works better for small- to moderate-size datasets.

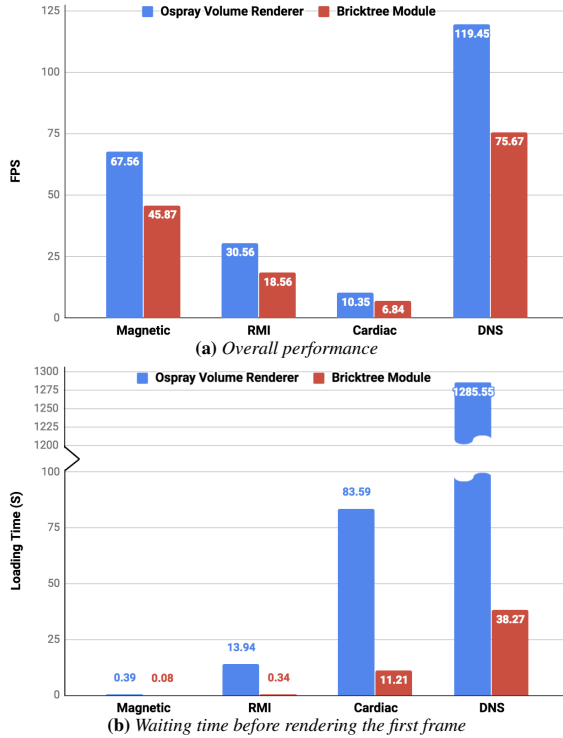


**Figure 6:** A comparison of overall performance and loading time between existing OSPRay volume renderer and our Bricktree module. The evaluation was run on Bricktree with a brick size of 4.

## 6.2 Choice of Brick Size

A volume renderer’s domain decomposition method can have a large impact on the performance of the rendering pipeline [14]. Our design and implementation allow the user to easily set a custom brick size. We performed a set of experiments to discover how the brick size affects the tree generation time, tree size, loading time, streaming performance and overall framerate. Two datasets were tested: RMI (8.1 GB, int8), which is a sparse dataset, and DNS(450 GB, float), which is a very dense dataset.

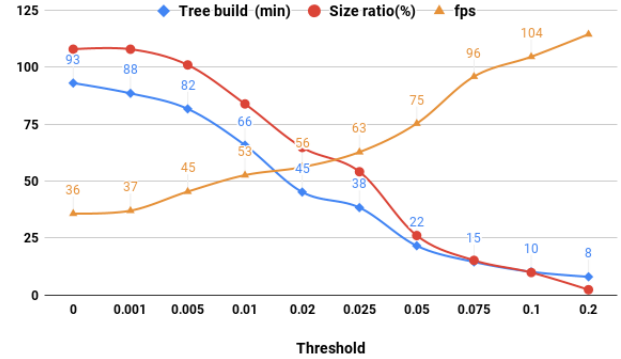
RMI / Brick Size	2	4	8	16
Tree Build (min)	1.61	1.49	1.34	1.96
Tree Size (GB)	7.80	5.90	7.10	9.60
Loading Time (s)	1.48	0.34	0.15	0.56
Stream Performance (s)	0.21	0.13	0.11	0.08
Framerate (fps)	10.56	18.56	10.75	7.78

DNS / Brick Size	2	4	8	16
Tree Build (min)	177.22	92.93	86.66	80.25
Tree Size (GB)	772	486	455	451
Loading Time (s)	92.26	38.27	9.3	7.67
Stream Performance (s)	0.18	0.16	0.13	0.08
Framerate (fps)	15.36	18.38	36.63	45.62

**Table 1:** An evaluation of tree build time, tree size, loading time, stream performance (s/1000 Valuebricks) and overall performance with different brick sizes on a sparse dataset (RMI) and a dense dataset (DNS). The evaluation was run on FSM. The tree build process was executed in parallel with eight processors.

Table 1 shows rendering performance with different brick sizes. As we know, the smaller Valuebrick size is more likely to be uni-



**Figure 7:** A comparison of tree build time, size ratio (tree size / volume size) and overall performance with different thresholds on the DNS dataset.

form in value [14]. In our unbalanced Bricktree, a Valuebrick that contains uniform values will not be further decomposed and stored by adopting a lossless fashion (mentioned in Section 3.3) and setting the threshold to the default value (0). Under this consideration, domain decomposition with a small brick size is more likely to yield a Bricktree with fewer Valuebricks. Therefore, a small brick size is more suitable for storage and probably fast traversal.

However, the results in Table 1 indicate a slightly different conclusion for different datasets. For a sparse dataset (e.g., RMI), a brick size of 4 produces a smaller tree and performs better than a brick size of 8 or 16. A brick size of 2 hampers performance and tree size, possibly due to an increased number of inner nodes resulting from greater tree depth.

For a dense dataset (e.g., DNS), where values vary in almost all cells, the output Bricktree is most likely a balanced tree. Hence, we found that a smaller brick size results in a larger tree size and longer construction time. From the perspective of streaming performance, a large brick size is preferable for disk performance. For instance, the size of a Valuebrick with a brick size 16 is 4 KB, which equals the size of a single memory page on FSM. Therefore, a brick size of 16 gives more a friendly memory access pattern. We observed that the streaming thread will influence rendering performance when many Valuebricks are requested. For performance reasons, we believe that a large Valuebrick size is more appropriate for visualizing dense datasets. Table 1 demonstrates that, for the DNS dataset, rendering performance is the best when a brick size of 16 is used.

Recall that a Bricktree is an octree when the brick size N is set to 2. It is shown from Table 1 that a Bricktree with an appropriate brick size outperforms an octree in terms of framerate, tree size, tree construction time, and loading time.

## 6.3 Bricktree Compression

In Section 3.3, we described how a threshold could be specified in order to collapse a specific input region of volume during the hierarchy generation. By using the default value 0, we produced a lossless hierarchical representation of the volume. Section 6.2 indicates that this lossless compression is satisfactory for a sparse dataset since regions with uniform values are collapsed. However, a lossy representation is generated if the threshold is set to a positive value. Figure 7 displays Bricktree build time, the ratio of the Bricktree’s size to raw volume and the rendering performance given different thresholds over the DNS dataset. The build time and tree size drop dramatically when the threshold is increased, and the rendering performance improves significantly. A detailed quantitative analysis of the accuracy of the output image over different thresholds is beyond the scope of this paper. However, Figure 8 depicts the output image of the magnetic dataset rendered with four thresholds.

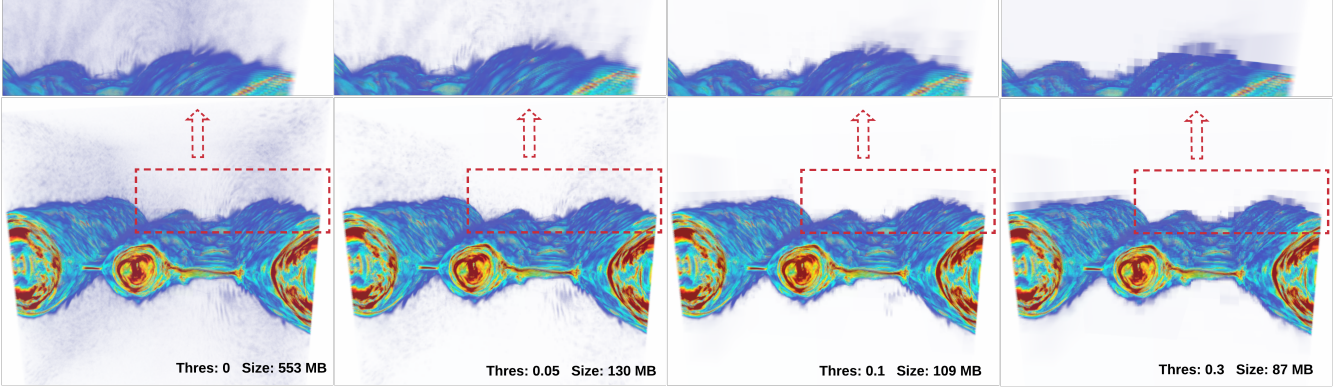


**Figure 8:** A comparison of the output image rendered with four thresholds on the magnetic dataset (512 MB). With an appropriate threshold, such as 0.05, we achieve significant performance improvement and produce a final image that is slightly different with ground truth (thres: 0).

Aside from the performance improvement, we observe that only a slight difference can be discerned in the final images if we select an appropriate threshold (e.g., 0.05) for the magnetic dataset. On the other hand, artifacts emerge when the data is visualized with a large threshold (e.g., 0.3).

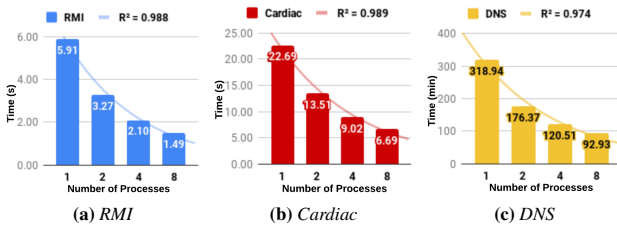


**Figure 9:** Tree build time by running the *ospRawToBrick* tool with different numbers of processes on three datasets. The brick size of the Bricktree is set to 4 in this evaluation.

#### 6.4 Bricktree Generation

Although hierarchy generation performance has drawn less attention than rendering performance, it is a significant bottleneck in real-world usage [14]. In this section, we evaluate the performance of the “*ospRawToBrick*” tool. Tree generation time, which benefits from the parallel build processes, drops dramatically by running multiple jobs simultaneously. Figure 9 shows hierarchy generation time with three datasets. For the RMI dataset, [14] claims that the generation time of their hierarchy structure takes about 13 minutes in the best case. However, with our solution, it only takes 1.49 seconds using eight processes.

#### 7 CONCLUSION

In this paper, we have presented a solution for interactive visualization of large volumes on multi-core CPU architectures. Our method is based on hierarchical representation and ray-guided progressive rendering that allows the user to view and explore hundreds of gigabytes of data without spending minutes or even hours waiting for data to load. Our solution is a significant improvement compared to the existing OSPRay volume renderer, which usually takes minutes or hours to load the data prior to rendering the first frame. Inspired by many recent renderers, we present a hierarchical data structure – a Bricktree – with a large branching factor and relatively low overhead. We have also evaluated and discussed the tradeoffs of the different parameters. Based on our experimental results, we conclude that

sparse datasets are best used with small brick sizes (e.g., 4), and dense datasets are best used with large brick sizes (e.g., 16).

Our data structure naturally facilitates compression. Using the Bricktree to create an easy-to-implement lossless compression scheme, we reduced the size of the RMI dataset from 8.1 GB to 5.9 GB with a brick size of 4 (Table 1). Furthermore, this scheme can easily be extended to support lossy compression.

Finally, we implemented our solution as a module for the OSPRay ray tracing framework. Since OSPRay is already interfaced with tools like ParaView and VisIt, users should have no difficulty putting our results into production.

In the future, we hope to further investigate data compression. For instance, Valuebricks are natural candidates for float-point data compression using ZFP [30]. Furthermore, a detailed quantitative analysis of how the lossy compression threshold affects final image quality should be performed. Eventually, we would like to integrate the Bricktree module into general-purpose visualization frameworks.

#### REFERENCES

- [1] J. Beyer, M. Hadwiger, and H. Pfister. A Survey of GPU-Based Large-Scale Volume Visualization. In *EuroVis - STARs*. The Eurographics Association, 2014. doi: 10.2312/eurovisstar.20141175
- [2] J. Beyer, M. Hadwiger, J. Schneider, W.-K. Jeong, and H. Pfister. Distributed terascale volume visualization using distributed shared virtual memory. In *Large Data Analysis and Visualization (LDAV), 2011 IEEE Symposium on*, pp. 127–128. IEEE, 2011.
- [3] H. Childs, M. A. Duchaineau, and K.-L. Ma. A scalable, hybrid scheme for volume rendering massive data sets. In *EGPGV*, pp. 153–161, 2006.
- [4] H. Childs, D. Pugmire, S. Ahern, B. Whitlock, M. Howison, G. H. Weber, E. W. Bethel, et al. Extreme scaling of production visualization software on diverse architectures. *IEEE Computer Graphics and Applications*, 30(3):22–31, 2010.
- [5] J. Clyne, P. Mininni, A. Norton, and M. Rast. Interactive desktop analysis of high resolution simulations: application to turbulent plume dynamics and current sheet formation. *New Journal of Physics*, 9(8):301, 2007.
- [6] R. H. Cohen, W. P. Dannevick, A. M. Dimits, D. E. Eliason, A. A. Mirin, Y. Zhou, D. H. Porter, and P. R. Woodward. Three-dimensional simulation of a richthmyer–meshkov instability with a two-scale initial perturbation. *Physics of Fluids*, 14(10):3692–3709, 2002.
- [7] C. Crassin, F. Neyret, and S. Lefebvre. *Interactive gigavoxels*. PhD thesis, INRIA, 2007.
- [8] C. Crassin, F. Neyret, S. Lefebvre, and E. Eisemann. Gigavoxels: Ray-guided streaming for efficient and detailed voxel rendering. In *Proceedings of the 2009 symposium on Interactive 3D graphics and games*, pp. 15–22. ACM, 2009.

- [9] S. Eilemann, M. Makhinya, and R. Pajarola. Equalizer: A scalable parallel rendering framework. *IEEE transactions on visualization and computer graphics*, 15(3):436–452, 2009.
- [10] K. Engel. CERA-TVr: A framework for interactive high-quality teravoxel volume visualization on standard PCs. In *Large Data Analysis and Visualization (LDAV), 2011 IEEE Symposium on*, pp. 123–124. IEEE, 2011.
- [11] W. Feng, W. Gang, P. Deji, L. Yuan, Y. Liuzhong, and W. Hongbo. A parallel algorithm for viewshed analysis in three-dimensional digital earth. *Computers and Geosciences*, (75):57–65, 2015.
- [12] B. Ferster. *Interactive visualization: Insight through inquiry*. MIT Press, 2012.
- [13] T. Fogal, H. Childs, S. Shankar, J. Krüger, R. D. Bergeron, and P. Hatcher. Large data visualization on distributed memory multi-GPU clusters. In *Proceedings of the Conference on High Performance Graphics*, pp. 57–66. Eurographics Association, 2010.
- [14] T. Fogal, A. Schiewe, and J. Krüger. An analysis of scalable GPU-based ray-guided volume rendering. In *Large-Scale Data Analysis and Visualization (LDAV), 2013 IEEE Symposium on*, pp. 43–51. IEEE, 2013.
- [15] E. Gobbetti, F. Marton, and J. A. I. Guitián. A single-pass GPU ray casting framework for interactive out-of-core rendering of massive volumetric datasets. *The Visual Computer*, 24(7-9):797–806, 2008.
- [16] F. Guo, H. Li, W. Daughton, and Y.-H. Liu. Formation of hard power laws in the energetic particle spectra resulting from relativistic magnetic reconnection. *Physical Review Letters*, 113(15):155005, 2014.
- [17] M. Hadwiger, A. K. Al-Awami, J. Beyer, M. Agus, and H. Pfister. SparseLeap: Efficient Empty Space Skipping for Large-Scale Volume Rendering. *IEEE transactions on visualization and computer graphics*, 24(1):974–983, 2018.
- [18] M. Hadwiger, J. Beyer, W.-K. Jeong, and H. Pfister. Interactive volume exploration of petascale microscopy data streams using a visualization-driven virtual memory approach. *IEEE Transactions on Visualization and Computer Graphics*, 18(12):2285–2294, 2012.
- [19] M. Hadwiger, F. Laura, C. Rezk-Salama, T. Höllt, G. Geier, and T. Papel. Interactive volume exploration for feature detection and quantification in industrial ct data. *IEEE Transactions on Visualization and Computer Graphics*, 14(6):1507–1514, 2008.
- [20] M. Howison, E. W. Bethel, and H. Childs. Hybrid parallelism for volume rendering on large-, multi-, and many-core systems. *IEEE Transactions on Visualization and Computer Graphics*, 18(1):17–29, 2012.
- [21] D. Keim, H. Qu, and K.-L. Ma. Big-data visualization. *IEEE Computer Graphics and Applications*, 33(4):20–21, 2013.
- [22] P. Klacansky. Open scientific visualization datasets, August 2018.
- [23] A. Knoll, S. Thelen, I. Wald, C. D. Hansen, H. Hagen, and M. E. Papka. Full-resolution interactive CPU volume rendering with coherent BVH traversal. In *Visualization Symposium (PacificVis), 2011 IEEE Pacific*, pp. 3–10. IEEE, 2011.
- [24] A. Knoll, I. Wald, S. Parker, and C. Hansen. Interactive isosurface ray tracing of large octree volumes. In *Interactive Ray Tracing 2006, IEEE Symposium on*, pp. 115–124. IEEE, 2006.
- [25] J. Krüger and R. Westermann. Acceleration techniques for GPU-based volume rendering. In *Proceedings of the 14th IEEE Visualization 2003 (VIS'03)*, p. 38. IEEE Computer Society, 2003.
- [26] S. Kumar, V. Vishwanath, P. Carns, B. Summa, G. Scorzelli, V. Pasucci, R. Ross, J. Chen, H. Kolla, and R. Grout. PIDX: Efficient parallel I/O for multi-resolution multi-dimensional scientific datasets. In *2011 IEEE International Conference on Cluster Computing*, pp. 103–111. IEEE, 2011.
- [27] S. Lefebvre, S. Hornus, F. Neyret, et al. Octree Textures on the GPU. *GPU gems*, 2:595–613, 2005.
- [28] M. Levoy. Efficient ray tracing of volume data. *ACM Transactions on Graphics (TOG)*, 9(3):245–261, 1990.
- [29] W. Li, K. Mueller, and A. Kaufman. Empty space skipping and occlusion clipping for texture-based volume rendering. In *Proceedings of the 14th IEEE Visualization 2003 (VIS'03)*, p. 42. IEEE Computer Society, 2003.
- [30] P. Lindstrom. Fixed-rate compressed floating-point arrays. *IEEE transactions on visualization and computer graphics*, 20(12):2674–2683, 2014.
- [31] R. D. Moser, J. Kim, and N. N. Mansour. Direct numerical simulation of turbulent channel flow up to  $Re = 590$ . *Physics of fluids*, 11(4):943–945, 1999.
- [32] T. Peterka, H. Yu, R. Ross, and K.-L. Ma. Parallel Volume Rendering on the IBM Blue Gene/P. In *Eurographics Symposium on Parallel Graphics and Visualization*. The Eurographics Association, 2008. doi: 10.2312/EGPGV/EGPGV08/073-080
- [33] M. Pharr and W. R. Mark. ISPC: A SPMD compiler for high-performance CPU programming. In *Innovative Parallel Computing (InPar)*, 2012, pp. 1–13. IEEE, 2012.
- [34] O. Procopiu, P. K. Agarwal, L. Arge, and J. S. Vitter. Bkd-tree: A dynamic scalable kd-tree. In *International Symposium on Spatial and Temporal Databases*, pp. 46–65. Springer, 2003.
- [35] S. Rusinkiewicz and M. Levoy. Qsplat: A multiresolution point rendering system for large meshes. In *Proceedings of the 27th annual conference on Computer graphics and interactive techniques*, pp. 343–352. ACM Press/Addison-Wesley Publishing Co., 2000.
- [36] M. Smelyanskiy, D. Holmes, J. Chhugani, A. Larson, D. M. Carmean, D. Hanson, P. Dubey, K. Augustine, D. Kim, A. Kyker, et al. Mapping high-fidelity volume rendering for medical imaging to CPU, GPU and many-core architectures. *IEEE transactions on visualization and computer graphics*, 15(6), 2009.
- [37] I. Wald. ISPC Bag of Tricks Part 3: Addressing 64-bit arrays in 32-bit addressing mode, Nov 2018.
- [38] I. Wald, H. Friedrich, G. Marmitt, P. Slusallek, and H.-P. Seidel. Faster isosurface ray tracing using implicit kd-trees. *IEEE Transactions on Visualization and Computer Graphics*, 11(5):562–572, 2005.
- [39] I. Wald, G. P. Johnson, J. Amstutz, C. Brownlee, A. Knoll, J. Jeffers, J. Günther, and P. Navratil. OSPRay—a CPU ray tracing framework for scientific visualization. *IEEE transactions on visualization and computer graphics*, 23(1):931–940, 2017.
- [40] I. Wald, P. Slusallek, C. Benthin, and M. Wagner. Interactive rendering with coherent ray tracing. In *Computer graphics forum*, vol. 20, pp. 153–165. Wiley Online Library, 2001.
- [41] I. Wald, S. Woop, C. Benthin, G. S. Johnson, and M. Ernst. Embree: a kernel framework for efficient CPU ray tracing. *ACM Transactions on Graphics (TOG)*, 33(4):143, 2014.
- [42] F. Wang, W. Li, S. Wang, and C. Johnson. Association rules-based multivariate analysis and visualization of spatiotemporal climate data. *ISPRS International Journal of Geo-Information*, 7(7):266, 2018.
- [43] F. Wang, I. Wald, Q. Wu, W. Usher, and C. R. Johnson. CPU Isosurface Ray Tracing of Adaptive Mesh Refinement Data. *IEEE Transactions on Visualization and Computer Graphics*, 2018.
- [44] Q. Wu, W. Usher, S. Petruzza, S. Kumar, F. Wang, I. Wald, V. Pasucci, and C. D. Hansen. VisIt-OSPRay: Toward an Exascale Volume Visualization System. In *EGPGV*, pp. 13–23, 2018.